A Murine Model for the Transition of *Streptococcus pneumoniae* from Asymptomatic Colonizer to Systemic Pathogen

Basma H. Joma[*1, 2], Nalat Siwapornchai[*1], Vijay K. Vanguri[3], Anishma Shrestha[1], Sara E. Roggensack[1, 4], Bruce A. Davidson[5], Albert K. Tai[6], Anders P. Hakansson[7], Simin N. Meydani[8], John M. Leong[#1] and Elsa N. Bou Ghanem[#9]

* Co-first authors; B.H.J. and N.S. contributed equally to this work; the order of names was chosen alphabetically

Co-corresponding authors

[1] Department of Molecular Biology and Microbiology at Tufts University School of Medicine, Boston, Massachusetts, USA

[2] Graduate Program in Immunology, Tufts Graduate School of Biomedical Sciences, Boston, USA

[3] UMass Memorial Health Care, University of Massachusetts Medical School, Worcester, Massachusetts, USA

[4]Graduate Program in Molecular Microbiology, Tufts Graduate School of Biomedical Sciences, Boston, USA

[5] Department of Anesthesiology, University at Buffalo School of Medicine, Buffalo, New York, USA

[6]Department of Immunology, Tufts University School of Medicine, Boston, Massachusetts, USA

[7] Department of Translational Medicine, Lund University, Malmö, Sweden

[8] Jean Mayer USDA Human Nutrition Research Center on Aging at Tufts University, Boston, Massachusetts, USA

24 [9]Department of Microbiology and Immunology, University at Buffalo School of Medicine,
25 Buffalo, New York, USA

26 Running Title: Murine Model of Influenza-Pneumococcal Co-infection

27 # Address correspondence and reprint requests to John M. Leong (J.M.L.), Department of
28 Molecular Biology and Microbiology, Tufts University School of Medicine, 136 Harrison
29 Avenue, Boston, MA 02114 and Elsa Bou Ghanem (E.N.B.G.), Department of Microbiology
30 and Immunology, University at Buffalo School of Medicine, 955 Main Street, Buffalo, New
31 York, USA. E-mail addresses: john.leong@tufts.edu (J.M.L.) and elsaboug@buffalo.edu
32 (E.N.B.G.)

33

34 Keywords: Co-infection, secondary bacterial pneumonia, *Streptococcus pneumoniae*,
35 Influenza A, colonization, aging, neutrophils, inflammation

36

37

38

39

40

41

42

43

44

45

46

47

48

ABSTRACT

Streptococcus pneumoniae (pneumococcus) resides asymptomatically in the nasopharynx but, as a pathobiont, can progress from benign colonizer to lethal pulmonary or systemic pathogen. Both viral infection and aging are risk factors for serious pneumococcal infections. Previous work established a murine model that featured the movement of pneumococcus from the nasopharynx to the lung upon nasopharyngeal inoculation with influenza A virus (IAV) but did not fully recapitulate the severe disease associated with human co-infection. We built upon this model by establishing pneumococcal nasopharyngeal colonization in mice, then inoculating both the nasopharynx and lungs with IAV. In young (2 months) mice, co-infection triggered bacterial dispersal from the nasopharynx into the lungs, pulmonary inflammation, concomitant disease and mortality in a fraction of mice. Although neutrophils are critical for pneumococcal clearance, IAV infection was associated with inefficient killing of pneumococci by neutrophils *ex vivo* and these cells were dispensable for host resistance during co-infection. In old mice (20-22 months), co-infection resulted in earlier and more severe disease compared to young mice. Aging was not associated with greater bacterial spread from the nasopharynx to the lungs or bloodstream. Rather, old mice displayed a more rapid proinflammatory cytokine response, earlier pulmonary neutrophil influx, lung damage and abrogated neutrophil function. Thus, in this model, IAV fosters the transition of pneumococci from commensals to pathogens through modifying bacterial behavior in the nasopharynx, enhancing pulmonary infection, and compromising neutrophil function. This model faithfully replicates age-associated susceptibility and can provide insight into factors that influence pathobiont behavior in different hosts.

73 **INTRODUCTION**

74 *Streptococcus pneumoniae* (pneumococcus) is a Gram-positive pathobiont that
75 typically resides asymptomatically in the nasopharynx of healthy individuals (1). It is
76 hypothesized *S. pneumoniae* establishes an asymptomatic biofilm on the nasopharyngeal
77 epithelium by attenuating the production of virulence factors and concomitant inflammation
78 (2-5). However, when immunity is compromised, a common occurrence in aging (6),
79 pneumococci can cause serious disease such as otitis media, pneumonia, meningitis and
80 bacteremia (7). In humans, pneumococcal carriage is believed to be a prerequisite to
81 invasive disease (8, 9). Bacterial isolates from invasive infections are genetically identical
82 to those found in the nasopharynx of patients (9); this and other longitudinal studies have
83 led to the suggestion that invasive disease often involves pneumococcal carriage in the
84 upper respiratory tract (8, 9).

85 The rate of reported colonization is quite variable among adults and is confounded
86 by differences in detection methods, but colonization may be more prevalent in the elderly
87 (10). A meta-analysis of twenty nine published studies found that in individuals above 60
88 years of age, conventional culture showed 0-39% carriage, while 3-23% carriage was
89 detected by molecular methods (11). Importantly carriage was higher among nursing home
90 residents (11). In older adults, conventional culture methods estimated carriage to be <5%
91 (12-14) but more recent data from European studies using molecular detection methods
92 indicated that carriage in the elderly ranges from 10-22% (10, 15-17). Thus, carriage rates
93 may be much higher than what was previously estimated in elderly individuals (12-14).

94 Advanced age increases the risk of invasive pneumococcal disease and
95 pneumococcal pneumonia (7). Aging is associated with immunosenescence, the overall
96 decline in immunity that accompanies aging as well as inflammaging, a low-grade chronic

97 inflammation that render the elderly more susceptible to pulmonary infections (18).
98 Polymorphonuclear leukocytes (PMNs), also known as neutrophils, are a crucial
99 determinant of age-related susceptibility to primary pneumococcal infection (19). These
100 cells are required to control bacterial burden at the start of infection (20-22). However,
101 aging is accompanied by impaired PMN anti-bacterial function (23, 24). In addition, aged
102 hosts experience exacerbated PMN pulmonary influx during primary pneumococcal
103 pneumonia (19, 25, 26), and persistence of PMNs in the airways beyond the first few days
104 leads to tissue destruction and systemic spread of infection (27, 28).

105 In addition to advanced age, epidemiological and experimental data show that
106 invasive pneumococcal infections are strongly associated with viral infection (29-31). The
107 risk of pneumococcal pneumonia is enhanced 100-fold by influenza A virus (IAV) infection
108 (32), resulting in the seasonal peak of pneumococcal disease during influenza outbreaks
109 (33). Further, *S. pneumoniae* is historically among the most common etiologies of
110 secondary bacterial pneumonia following influenza and associated with the most severe
111 outcomes (30, 34-36). Symptoms of secondary bacterial pneumonia include cough,
112 dyspnea, fever, muscle aches and when severe result in hospitalizations, respiratory
113 failure, mechanical ventilation, and can lead to death (30, 34-36).

114 IAV commonly infects the upper respiratory tract, and at this location viral infection
115 can enhance the nutritional environment for pneumococcus in the nasopharynx, leading to
116 greater bacterial loads and/or higher rates of bacterial acquisition (4, 37). IAV can also
117 directly bind the pneumococcal surface and enhance bacterial binding to the pulmonary
118 epithelium leading to increased colonization (38). In addition, viral infection of the
119 pulmonary epithelium induces the release of host components, such as adenosine
120 triphosphate and norepinephrine, that are sensed by biofilm-associated pneumococci,

121 triggering both the production of pneumococcal virulence factors and the dispersal of
122 bacteria (4, 37, 39, 40). This in turn facilitates bacterial spread to and colonization of the
123 lower respiratory tract (4). Murine models featuring sequential lung challenge with IAV first
124 followed by pneumococcus show the virus can also compromise pulmonary immune
125 defense against pneumococcus (29, 34, 41). In these models, IAV alters both the lung
126 environment and the immune response to enhance subsequent bacterial colonization and
127 tissue damage. For example, IAV pre-infection increases mucus production and fibrosis
128 and dysregulates ciliary function (34, 42, 43), thus impairing mechanical clearance of
129 invading bacteria. Viral enzymes, along with virus-elicited inflammation, result in the
130 exposure of epithelial proteins that promote pneumococcal adherence to and invasion of
131 host cells (41, 44-46). Further, IAV triggers type I and II interferon (IFN) responses that
132 impair both the recruitment and antibacterial function of phagocytes key to defense against
133 pneumococcus (47-50). The combined tissue damage and the compromise in immune
134 function render the lung more permissive for invasive *S. pneumoniae* infection (34, 45, 47).
135 These studies indicate that bacterial-viral synergy is multi-factorial and can occur at
136 different sites with the host.

137 Notably, advanced age and IAV infection appear to synergistically enhance
138 susceptibility to pneumococcal lung infections (6, 18, 51, 52). Indeed, individuals ≥ 65
139 years old account for 70-85% of deaths due to pneumonia and influenza (52). Interestingly,
140 elderly individuals with influenza-like symptoms were reported to have an increased
141 pneumococcal carriage rate of 30% (53). In animal models in which bacteria are directly
142 instilled into the lungs following influenza infection, aging is associated with increase
143 susceptibility of secondary pneumococcal pneumonia (51). Age-dependent changes in the
144 expression of key components of innate immune signaling contribute to disease in this co-

145 infection model (51). However, the factors, including those that are age-dependent, that
146 trigger the transition of pneumococci from benign colonizer to pathogen are poorly defined,
147 in part because small animal models that recapitulate the transition from asymptomatic
148 colonization to overt clinical illness are lacking.

149 Insight into events that occur in both the nasopharynx and lung and contribute to the
150 heightened susceptibility of the aged to serious disease upon pneumococcal/IAV
151 coinfection is needed to develop better therapeutic and preventative approaches. A current
152 murine model for the spread of nasopharyngeal pneumococci to the lung after viral
153 infection of the upper respiratory tract relies on initial bacterial colonization of the
154 nasopharynx followed by viral infection, but does not recapitulate the severe signs of
155 human clinical disease (4). To better investigate the transition of *S. pneumoniae* from
156 asymptomatic colonizers to invasive pathogens following IAV infection, as well as the
157 effect of host age on the disease process, we built upon this mouse model of *S.*
158 *pneumoniae/*IAV co-infection. The enhanced model incorporates the sequential
159 introduction of bacteria and virus and recapitulates the severe and age-exacerbated
160 clinical disease observed in humans.

161

162 **RESULTS**

163 **Intranasal IAV inoculation of mice pre-colonized with *S. pneumoniae* strain TIGR4**
164 **does not result in disease.**

165 Biofilm-grown *S. pneumoniae* are relatively less virulent and thus adapted to host
166 colonization rather than disease (2-4). A previously established murine model in
167 BALB/cByJ mice utilizes biofilm-grown *S. pneumoniae* strains D39 and 19F EF3030 to
168 establish heavy carriage in the nasopharynx (4). Then, two days after bacterial inoculation,

169 IAV is introduced into the nasal cavity and results in the spread of pneumococci from the
170 nasopharynx (NP) to the lung (4). We first recapitulated this model with *S. pneumoniae*
171 strain TIGR4, an invasive serotype 4 strain (54, 55) that we previously found to be highly
172 virulent in aged C57BL/6 mice (19). We intranasally (i.n.) inoculated young (8-10 weeks)
173 C57BL/6 (B6) mice with $1x10^6$ colony forming units (CFU) of biofilm-generated *S.*
174 *pneumoniae* TIGR4 by delivering the bacteria in 10 µl (a volume that is unlikely to
175 inoculate the lung (56)) to the nares of non-anesthetized mice. Forty-eight hours later,
176 mice were i.n. inoculated with 10 µl containing 20 PFU of Influenza A (IAV) virus PR8.
177 (See Fig. S1A for general scheme). Control groups of mice were either infected with *S.*
178 *pneumoniae* or IAV alone as controls. However, under these conditions, mice did not
179 display signs of sickness, nor did bacteria spread into the lungs after seven days (not
180 shown).
181 To increase the likelihood of clinical disease, we repeated the experiment with a
182 five-fold higher ($5x10^6$ CFU) dose of bacteria and a 25-fold higher dose (500 PFU) of IAV.
183 Similar to earlier reports for other *S. pneumoniae* strains (D39 and 19F) (4), IAV co-
184 infection resulted in a 10-fold increase in *S. pneumoniae* TIGR4 in the nasal lavage fluid at
185 2 days post-IAV infection (Fig. S1B). In addition, IAV co-infection was associated with the
186 detection of bacteria in the lungs of 40% of mice, compared to none in the control group
187 infected with *S. pneumoniae* TIGR4 alone. This trend is consistent with the previous
188 BALB/cByJ mice model of coinfection (4), but did not reach statistical significance.
189 Furthermore, co-infection was not associated with weight loss when assessed over the
190 course of 4 days post-infection (Fig. S1C). We also scored mice for clinical signs of the
191 disease based on weight loss, activity, posture and breathing and ranging from healthy
192 [score = 0] to moribund [score = 25] and requiring euthanasia if the score was >9 as

193 previously described (57). As secondary pneumonia can occur several days following IAV
194 (41), we monitored the disease course up to 7 days, but did not detect disease symptoms
195 or death in any of the co-infected mice (100% survival and 0 daily clinical score for all
196 mice). Therefore, despite promoting bacterial dispersal from the nasopharynx into the
197 lungs, this model of *S. pneumoniae* TIGR4/IAV coinfection did not result in overt clinical
198 signs of disease.
199
200 **Combined intranasal/intratracheal IAV inoculation of *S. pneumoniae*-colonized mice**
201 **results in bacterial dissemination and disease**
202 IAV infection is not restricted to the upper respiratory tract, and can cause viral
203 pneumonia in a significant fraction of infected individuals (58, 59) that is likely to be crucial
204 for creating an environment in the lungs that is more permissive for bacterial infection (29,
205 34, 41). Indeed, viral lung infection diminishes pulmonary defenses against *S. pneumoniae*
206 and promotes secondary bacterial pneumonia (34, 41, 44-50). Delivery of IAV i.n. to
207 BALB/cByJ mice results in signs of viral pneumonia (4), but we found that pulmonary
208 access of inocula delivered via the nasopharynx is more restricted in B6 mice as compared
209 to BALB/c mice (unpublished observation), raising the possibility that the lack of disease
210 observed in co-infected B6 mice was due to the exclusive localization of virus in the nasal
211 cavity, with limited opportunity to alter systemic or pulmonary immunity.
212 To ensure delivery of IAV to both the nasopharynx and the lungs, we co-infected *S.*
213 *pneumoniae*-colonized B6 mice by delivering the virus by two routes. Mice were inoculated
214 i.n. with $5x10^6$ CFU of biofilm grown S. *pneumoniae* TIGR4 and 48 hours later infected not
215 only with 500 PFU IAV i.n., but also 20 PFU i.t. to ensure pulmonary infection (Fig. 1A). No
216 mice in a control group inoculated i.n. with *S. pneumoniae* alone lost weight (Fig 1B),

217 displayed clinical signs of sickness (Fig 1C), or died (Fig 1D). A second control group,
218 inoculated i.n. and i.t. with IAV alone displayed no disease until after day 4, when they
219 exhibited weight loss (Fig 1B) and began succumbing to viral infection (Fig 1D). In
220 contrast, inoculation of IAV to animals pre-colonized with *S. pneumoniae* caused a
221 bacterial/viral co-infection that resulted in weight loss (Fig. 1B), clinical symptoms (Fig. 1C)
222 and death (Fig. 1D) that were detected starting day 2 post IAV introduction. At this time
223 point, a higher fraction of co-infected mice displayed signs of disease as compared to
224 controls infected with IAV only (40% vs 64%), and disease was more severe in sick mice,
225 although this did not reach statistical significance. In addition, the overall survival rate
226 among co-infected mice was significantly lower than mice singly infected with *S.*
227 *pneumoniae* alone (Fig. 1D). These signs of exacerbated disease were associated with
228 significantly higher bacterial burdens in the nasopharynx as well as translocation of *S.*
229 *pneumoniae* into the lung in comparison to mice colonized with the bacteria or mice
230 infected with IAV alone (Fig. 1E). These findings demonstrated that the new co-infection
231 model leads to disease in a fraction of young healthy mice, which may increase the
232 likelihood of detecting enhanced susceptibility in vulnerable hosts.
233

234 **PMN depletion has no significant effect on the course of disease during IAV/*S.***
235 ***pneumoniae* co-infection**

236 We previously found that in primary pneumococcal pneumonia, PMNs are required
237 to control bacterial numbers early in the infection process; however their persistence in the
238 lungs is detrimental to the host and can promote the infection at later time points (20). To
239 address the role of PMNs during co-infection, we treated young mice with PMN-depleting
240 anti-Ly6G antibody (1A8) one day prior to pneumococcal colonization and throughout the

241 co-infection (based on timeline in Figure 1A). We then confirmed that the cells were
242 depleted by staining with the RB6 antibody followed by flow cytometry (see materials and
243 methods). Following infection, we measured bacterial burden, weight loss, clinical score
244 and survival over time. Surprisingly, PMN depletion had no effect on bacterial burdens in
245 the nasopharynx or bacterial spread to the lungs or blood following co-infection (Fig 2A
246 and B). PMN-depletion was not associated with any significant differences in weight loss
247 as compared to the control group (Fig. 2C). Additionally, untreated controls and PMN-
248 depleted mice had comparable clinical signs of sickness at 18 hours and 48 hours post
249 IAV infection (Fig. 2D). Lower survival was observed in the depletion group, where only
250 25% survived to day 7 compared to ~43% survival from untreated controls; however, this
251 difference was not statistically significant (Fig. 2E). In conclusion, PMN depletion prior to
252 infection appeared to have a slight but not significant effect on the course of co-infection in
253 young mice in this model.
254
255 **Aging increases susceptibility to IAV/*S. pneumoniae* co-infection.**
256 We next tested if the new co-infection mouse model (Fig. 1A) recapitulates the age-
257 associated increase in susceptibility to secondary pneumococcal pneumonia. Old (20-24
258 months) B6 mice were inoculated i.n. with $5x10^6$ CFU of biofilm grown S. *pneumoniae*
259 TIGR4 and 48 hours later were infected with 500 PFU IAV i.n. plus 20 PFU i.t. When
260 compared to young co-infected controls, old mice displayed significantly more severe signs
261 of disease, as indicated by a higher average clinical score (Fig. 3A). While seven of 16
262 (43.75%) young mice showed clinical symptoms (i.e., clinical score greater than 1; Fig.
263 3A), all 13 old mice showed at least some degree of illness by day 2 post co-infection (p =
264 0.0012, by Fisher's exact test). Furthermore, whereas only 25% (4 out of 16) young mice

265 had a clinical score greater than 2, which is indicative of more severe disease, 92% (12 out
266 of 13) aged mice fell into this category (p = 0.005, by Fisher's exact test). In addition, old
267 mice died at a significantly accelerated rate. By day 2 post co-infection, 60% of old mice
268 had succumbed to the infection compared to only 25% of young mice. Differences in
269 survival were observed at each successive time point, and at the end of the experiment on
270 day 8, only 14% of old mice remained alive compared to 50% of young mice (Fig. 3B).
271 Importantly, the accelerated death observed in co-infected old mice was not observed in
272 old mice infected with *S. pneumoniae* alone or IAV alone (Fig S2).
273 We next tested whether these differences could be attributed to increased bacterial
274 loads in the nasopharynx, lungs, or blood. As old mice got sicker at earlier time points post
275 IAV co-infection, with the majority succumbing by day 4, we compared bacterial burden
276 across age groups at 18 and 48 hours post IAV co-infection. We found no significant
277 differences in the numbers of pneumococci in nasopharyngeal washes, pulmonary
278 homogenates, or blood at either time point (Fig 3C-E). Taken together, these findings
279 suggest that with aging there is an increased susceptibility to co-infection and an
280 accelerated course of disease that could not be attributed to a more rapid bacterial
281 dissemination or higher bacterial loads in the nasopharynx, lung, or bloodstream.
282
283 **Aging is associated with more rapid lung inflammation.**
284 We previously found that mice suffering from exacerbated PMN-mediated
285 pulmonary inflammation during pneumococcal pneumonia did not display higher bacterial
286 burdens in their lungs (27) despite a higher likelihood of severe disease (19, 20, 27). To
287 test whether PMN influx was higher in old co-infected mice, we measured the percentage
288 and number of pulmonary PMNs ($Ly6G^+$) by flow cytometry. We found that old mice had

289 significantly (6-fold) higher percentages and numbers of PMNs in their lungs as compared
290 to young controls at 18 hours post co-infection (Fig 4A). By 48 hours, although PMN
291 percentages and numbers appeared to be higher in young mice, the differences were not
292 statistically significant (Fig. 4A and B). Macrophages, which are important for host
293 resistance to *S. pneumoniae/IAV* co-infection (49) and display age-driven changes (60,
294 61), displayed no significant age-dependent differences in either percentage or number
295 (Fig. S3).

296 Next we tested the levels of inflammatory cytokines in co-infected young vs old
297 mice. No significant differences between age groups were detected in baseline
298 (uninfected) levels of any of the cytokines tested between the age groups (Fig 4B and not
299 shown). However, consistent with the enhanced PMN influx at 18 h post-infection in aged
300 mice, old mice had significantly higher levels of IL-10, IL-2, IL-1β and TNFα (Fig 4B)
301 compared with young mice. Levels of IL-12p70, IL-17, IL-6 and IFNγ, were slightly but not
302 significantly elevated 18 hours post co-infection (Fig S4A). By 48 hours there were no
303 significant differences between young and old mice in cytokine levels except for IFNγ,
304 which was higher in young mice (Fig S4B).

305 To determine if the pulmonary inflammation was associated with lung damage, we
306 analyzed H&E stained lung sections for alveolar congestion, hemorrhage, alveolar
307 thickness, neutrophils and lymphocytic infiltration (Fig. 4C). We found that the alveolar
308 spaces of both uninfected old and young mice were clear and free of inflammatory or red
309 blood cells (Fig. 4C). Similarly, at 18h hours post co-infection, the lungs of young mice did
310 not show any overt signs of disease (Fig. 4C). However, co-infected old mice had
311 significant pathology in the lungs by 18 hours post infection, including a loss of alveolar
312 architecture, and spotty inflammation consisting of infiltrates composed of neutrophils,

313 alveolar macrophages and mononuclear cells that were mixed with red blood cells (Fig.
314 4C). At 48 hours post-infection, there were clear signs of lung pathology in both young and
315 old co-infected mice (Fig. 4C). Taken together, these findings demonstrate that aging is
316 associated with earlier pulmonary inflammation and damage following co-infection, which
317 may account for the accelerated death observed in this mouse group.
318
319 **Aging and IAV infection diminish the ability of PMNs to kill *S. pneumoniae ex vivo*.**
320 Aged, co-infected mice experience an accelerated rate of pulmonary inflammation
321 but bacterial loads in the lungs of aged mice were not lower than in young mice, indicating
322 that PMN infiltration is not associated with bacterial clearance. Both aging (24) and IAV
323 infection (62) have been reported to diminish antibacterial function of PMNs. To assess the
324 ability of PMNs to kill *S. pneumoniae* in our co-infection model, we used a well-established
325 opsonophagocytic (OPH) killing assay (19, 63). We first compared the bactericidal activity
326 of bone marrow-derived PMNs from young or aged mice. The percentage of bacteria killed
327 upon incubation with PMNs was determined by comparing surviving CFU to no PMN
328 control reactions. We found that as previously reported for humans (23) and mice (24) the
329 ability of PMNs isolated from uninfected old mice to kill pneumococci was reduced 5-fold
330 compared to young controls (Fig. 5).
331 We next examined the bactericidal activity of PMNs isolated from young or old mice
332 2-days after i.t./i.n. IAV inoculation. As previously reported (47-50), PMNs from young IAV
333 infected mice had a slight (2-fold) but significant reduction in their ability to kill
334 pneumococci as compared to PMNs from uninfected controls (Fig. 5). Strikingly, IAV
335 infection abolished the ability of PMNs from old mice to kill *S. pneumoniae*; instead, PMNs
336 from IAV infected old mice promoted bacterial growth instead of death (Fig. 5). These

337 findings suggest that IAV infection completely abrogates the ability of PMNs from old mice
338 to kill *S. pneumoniae.*
339
340 **DISCUSSION**
341 *S. pneumoniae* remains a leading cause of secondary bacterial pneumonia
342 following influenza A virus infection and is associated with severe disease (30, 34-36),
343 particularly in the elderly (52). The majority of *S. pneumoniae/*IAV co-infection studies have
344 delivered bacteria into the lungs of mice pre-infected with IAV to reveal changes in the host
345 lungs and immune response that are crucial for priming invasive pneumococcal disease
346 (34, 41, 44-50). In this study, to investigate the transition of *S. pneumoniae* from colonizer
347 to pathogen upon IAV co-infection, a process that has just started to be elucidated (4, 37),
348 we have developed a modified murine infection model that recapitulates this transition and
349 results in severe clinical disease. In a previously established model, female BALB/cByJ
350 mice were first colonized intra-nasally with biofilm-grown pneumococci and then infected
351 with IAV by delivering the virus to the nasopharynx (4, 40). This model showed that
352 changes in the host environment in response to viral infection triggers the dispersal of
353 pneumococci from colonizing biofilms and their spread to the lower respiratory tract (4).
354 Importantly, the dispersed bacteria expressed higher levels of virulence factors required for
355 infection, thus, rendering them pathogenic (4). When we used this model to co-infect male
356 C57BL/6 (B6) mice, we observed a significant increase in dispersed bacteria in the
357 nasopharynx, but no disease and only a transient presence of *S. pneumoniae* in the lungs
358 of B6 mice. This could be due to the differences in host susceptibility to bacterial infection
359 between the different mouse strains, which has been well described for *S. pneumoniae*
360 (64, 65) and other infections (66) or due to gender (67): Here we performed experiments in

361 male instead of female mice due to both the easier availability of aged male animals and
362 the documented higher rate of pneumococcal pneumonia in men compared to women (68,
363 69).

364 Previous work of pneumococcal inoculation of IAV-infected lungs showed viral
365 infection to be crucial for creating an environment in the lungs that is more permissive for
366 bacterial infection (41, 44-50). The relatively low bacterial burden in co-infected male B6
367 mice observed here upon IAV inoculation only by the i.n. route suggested that the lung
368 environment was not sustaining the bacteria. Therefore, we co-infected *S. pneumoniae*
369 colonized B6 mice with IAV by delivering the virus not only i.n. to infect the nasopharynx,
370 but also i.t. to ensure infection of the lungs. This modified model recapitulated the increase
371 in non-adherent pneumococci in the nasopharynx observed upon viral co-infection (4, 70,
372 71), and resulted in bacterial spread into the lungs and circulation that increased over time.
373 Importantly, this mode of dual infection recapitulated both the increased colonization
374 burden (72, 73) as well as the clinical signs of severe disease observed in humans (30, 34-
375 36), and resulted in death of approximately half of co-infected young controls.

376 Although the elderly are at higher risk for secondary pneumococcal pneumonia
377 following IAV infection, animal studies exploring this age-driven susceptibility to co-
378 infection are few (51, 74, 75). Here, using the modified model, we found that old mice were
379 significantly more susceptible to *S. pneumoniae/*IAV co-infection. Old mice displayed more
380 severe signs of disease as compared to young controls and the majority (>85%) failed to
381 survive the co-infection. This increased susceptibility in old mice was not linked to higher
382 bacterial dissemination from the nasopharynx, or greater establishment of infection in the
383 lungs or systemic spread into the circulation at the time points tested. Although we did not
384 directly measure viral loads, susceptibility to viral infection alone as measured by weight

385 loss, within the first 5 days following IAV was also similar between the age groups. Rather,
386 the age-driven susceptibility to co-infection was associated with earlier and more severe
387 pulmonary inflammation. Production of cytokines in the lungs has been reported in young
388 mice infected with *S. pneumoniae* 7 days post IAV (76). Further, old mice displayed
389 changes in the expression of pattern recognition receptors in the lungs leading to altered
390 inflammatory responses (51). Similar to previous studies (51), we found here that co-
391 infected old mice had higher levels of TNFα as compared to young controls. However, in
392 contrast to previous reports that found reduced NLRP3 inflammasome expression in the
393 lungs and lower production of IL-1β, we found higher levels of IL-1β in old mice as
394 compared to young controls. This may be accounted for by differences in expression of
395 bacterial factors. The expression of pneumolysin, which was found to activate NLRP3
396 inflammasomes and lead to production of IL-1β (77), was elevated in pneumococci
397 dispersed from biofilms upon IAV infection (78) and therefore may have primed the IL-1β
398 production we observed in old mice.

399 We previously found that PMNs were key determinants of disease during primary
400 pneumococcal pneumonia and are required to initially control bacterial numbers (20, 79).
401 Therefore, we explored here the role of PMNs in *S. pneumoniae/*IAV co-infection. Similar
402 to other studies, we found that PMNs are recruited to the lungs of co-infected young mice
403 (49). Previous reports indicate that the PMN-mediated anti-pneumococcal function in IAV-
404 infected mice (62) and humans (73) is progressively reduced over time. For example, in
405 mice, PMNs demonstrably contribute to host defense at 3 days but not at 6 days post-
406 infection (62). Nevertheless, PMN depletion showed that these cells are important for
407 control of bacterial transmission (80) and control of pulmonary bacterial numbers (49) in
408 IAV co-infected mice. In contrast, here we found that PMN depletion starting prior to

409 bacterial colonization and continuing throughout viral co-infection had no significant effect
410 on the number of dispersed *S. pneumoniae* in the nasopharynx or their spread to the lungs
411 and blood. In this model IAV may rapidly impair PMN function, and in fact, we found that
412 within 2 days following IAV infection, the ability of bone marrow-derived PMNs to kill *S.*
413 *pneumoniae* was significantly blunted in young mice. Alternatively, the apparent inability of
414 PMNs to limit bacterial numbers in this model could be due to the enhanced virulence of
415 pneumococci dispersed from the nasopharyngeal environment (4) compared to broth-
416 grown bacteria typically used in other models (62).

417 In this study we found that aging was associated with earlier influx of PMNs into the
418 lungs of co-infected mice. We previously demonstrated that excessive PMN influx into the
419 lungs is detrimental for the ability of old mice to control invasive disease following primary
420 pneumococcal pneumonia (19) and that PMN depletion 18 hours after infection boosted
421 host survival (20). Similarly, exacerbated PMN influx into the lungs of old mice singly
422 infected with IAV was associated with host mortality, and depletion of these cells six days
423 following viral infection significantly boosted host survival (81). Uncontrolled PMN influx
424 can result in tissue damage, disruption of gaseous exchange and pulmonary failure. In
425 fact, it was reported that in IAV singly infected old mice, PMNs mediated lung inflammation
426 and damage and their depletion reduced the levels of inflammatory IL-1β and TNFα (81).
427 Therefore, the early increase in these inflammatory cytokines and lung damage we
428 observed here in *S. pneumoniae/*IAV co-infected old mice may be driven by the elevated
429 levels of pulmonary PMNs.

430 In this model, aging was associated with significantly increased levels of pulmonary
431 IL-10 during *S. pneumoniae/*IAV confection as compared to young controls, which may
432 account for their enhanced susceptibility to co-infection. IL-10 was previously shown to

433 impair host resistance to *S. pneumoniae* following IAV infection (82). IL-10 levels were
434 elevated in co-infected young mice as compared to those singly infected with *S.*
435 *pneumoniae* and blocking this cytokine resulted in reduced bacterial numbers and
436 extended host survival (82). The elevated IL-10 may also account for the complete
437 inability of PMNs from IAV infected old mice to kill *S. pneumoniae.* We previously found
438 that IL-10 impairs PMN anti-bacterial function by inhibiting ROS production in response to
439 infection (79). Blocking this cytokine boosted PMN anti-bacterial function and importantly
440 restored resistance of vulnerable hosts to primary pneumococcal pneumonia (79).
441 In summary, here we modified existing murine models to establish an experimental
442 system that reflects the transition of *S. pneumoniae* from asymptomatic colonizer to
443 invasive pulmonary pathogen upon IAV co-infection. In this model, IAV triggers the
444 transition of a pathobiont from a commensal to a pathogenic state through modification of
445 bacterial behavior in the nasopharynx, enhancement of bacterial colonization in the lung,
446 and compromise of PMN-mediated anti-bacterial immunity. Importantly this model
447 recapitulates the susceptibility of aging to co-infections. Moving forward, this model can be
448 used to dissect the multiple phases of pneumococcal disease progression from
449 commensals to pathogens, which can help inform specialized treatment options (70)
450 tailored to the susceptible elderly population.
451
452 **MATERIALS AND METHODS**
453 **Mice.** Young (8-10 weeks) and aged (18-24 months) male C57BL/6 mice were purchased
454 from Jackson Laboratories (Bar Harbor, ME) and the National Institute of Aging. Mice were
455 housed in a pathogen-free facility at Tufts University. All procedures were performed in
456 accordance with Institutional Animal Care and Use Committee guidelines.

457

458 **Bacterial biofilms.** NCI-H292 mucoepidermoid carcinoma cells (H292) were grown in 24-
459 well plates in RPMI 1640 media with 10% FBS and 2mM L-glutamine until confluent. Cells
460 were washed with 1x PBS and fixed in 4% paraformaldehyde for 1 hour on ice. *S.*
461 *pneumoniae* TIGR4 (kind gift from Andrew Camilli) were grown on Tryptic Soy Agar plates
462 supplemented with 5% sheep blood agar (blood agar plates) overnight, then diluted and
463 grown in chemically defined liquid medium (CDM) (4, 40) supplemented with Oxyrase until
464 OD_{600nm} of 0.2. Bacteria were diluted 1:1000 in CDM and seeded on the fixed H292 cells.
465 The, bacteria/H292 cells were incubated at 34°C/ 5% CO_2 and media was changed every
466 12 hours. At 48 hours post-infection, the supernatant containing planktonic bacteria (non-
467 adherent to NCI-H292 cells) cells was discarded, the cells gently washed with PBS and
468 adherent biofilms collected in fresh CDM by vigorous pipetting. Biofilm aliquots were then
469 frozen at -80°C in the CDM with 25% (v/v) glycerol.

470

471 **Intranasal inoculation.** Before use, biofilm aliquots were thawed on ice, washed once and
472 diluted in PBS to the required concentration. The mice were restrained without anesthesia
473 and infected i.n. with 10µl ($5x10^6$ CFU) of biofilm grown *S. pneumoniae*. The inoculum was
474 equally distributed between the nostrils with a pipette. Bacterial titers were confirmed by
475 serial dilution and plating on blood agar plates. To ensure stable colonization of the biofilm
476 in the nasopharynx, groups of mice were euthanized at 18 and 48 hours post inoculation,
477 and the nasal washes and tissue were collected and plated on blood agar plate for
478 enumeration of *S. pneumoniae*.

479

480 **Viral infection.** The mouse-adapted H1N1 Influenza A virus PR8 (A/PR/8/34) was
481 obtained from Dr. Bruce Davidson (4, 40) and stored at -80℃. Before use, viral aliquots
482 were thawed on ice, diluted in PBS and used to inoculate mice. At 48 hours following
483 bacterial inoculation, mice were infected i.n. with 10µl of 500 plaque forming units (PFU) of
484 virus by pipetting the inoculum into the nostrils of non-anesthetized mice. Following i.n.
485 inoculation, mice were lightly anesthetized with isoflurane and challenged i.t. with 20 PFU
486 of virus in a 50µl volume pipetted directly into the trachea with the tongue pulled out to
487 facilitate delivery (20).
488
489 **Clinical scoring and bacterial burden.** Following co-infection, mice were monitored daily
490 and blindly scored for signs of sickness including weight loss, activity, posture and
491 breathing. Based on these criteria, the mice were given a clinical score of healthy [0] to
492 moribund [25] as previously described (57). Any mice displaying a score above 9 are
493 humanely euthanized in accordance with our protocol. Mice were euthanized at indicated
494 time points and the lung, nasal lavages and blood collected and plated on blood agar for
495 enumeration of bacterial loads, as previously described (20). For collection of sera, blood
496 was collected via cardiac puncture into Microtainer® tubes (BD Biosciences) and
497 centrifuged at 7607xg for 2 minutes to collect serum as per manufacturer's instructions.
498
499 **Depletion of PMNs.** Mice were intraperitoneally (i.p.) injected with 100µl (50µg/mouse) of
500 anti-Ly6G clone 1A8 (BD Biosciences) to deplete neutrophils. Mice were injected daily with
501 the depleting antibodies starting one day prior and ending two days after bacterial
502 inoculation, followed by every other day from day 1 post viral co-infection to the end of
503 each experiment. Treatment resulted in >90% neutrophil depletion as described below.

504

505 **Cell isolation and Flow Cytometry.** Mice lungs were harvested, washed in PBS, and
506 minced into small pieces. The sample was then digested for 45 minutes with RPMI 1640
507 1X supplemented with 10% FBS, 1 mg/ml Type II collagenase (Worthington, Lakewood,
508 NJ), and 50 U/ml deoxyribonuclease I to obtain a single-cell suspension as previously
509 described (20). The red blood cells were lysed using ACK lysis buffer (Gibco). Cells were
510 then stained with anti-mouse Ly6G clone 1A8 (BD Biosciences), F480 clone BM8
511 (BioLegend), CD11c clone N418 (eBioscience), and CD11b clone M1/70 (eBioscience).
512 For neutrophil depletion, cells isolated from the lungs at 18 and 48 h post co-infection were
513 also stained with either Ly6G clone 1A8 or RB6 clone RB6-8C5 (BioLegend) antibodies to
514 confirm cell depletion. The fluorescence intensities were measured on BD LSR II Flow
515 Cytometer at Tufts FACS Core Facility (Boston, MA) to capture at least 25,000 cells and
516 analyzed using FlowJo.

517

518 **Isolation of PMNs and Opsonophagocytic Killing Assay (OPH).** Femurs and tibias of
519 uninfected mice were collected and flushed with RPMI, supplemented with 10% FBS and 2
520 mM EDTA to obtain bone marrow cells. Neutrophils were isolated by density gradient
521 centrifugation, using Histopaque 1119 and Histopaque 1077 as previously described (83).
522 The neutrophils were resuspended in Hank's (Gibco) buffer/0.1% gelatin with no Ca+ or
523 Mg+ and tested for purity by flow cytometry using anti-Ly6G antibodies (eBioscience)
524 where 85-90% of enriched cells were Ly6G+. The ability of neutrophils to kill bacteria was
525 measured using a well-established opsonophagocytic (OPH) killing assay as previously
526 described (20). Briefly, 2.5×10^5 neutrophils were incubated in Hank's buffer/0.1% gelatin
527 with 10^3 CFU of *S. pneumoniae* pre-opsonized with 3% mouse sera. The reactions were

528 incubated in flat bottom 96-well non-binding plates for 45 minutes at 37°C. Each group
529 was plated on blood agar to enumerate viable CFU. Percent bacterial killing was
530 calculated in comparison to a no PMN control under the same conditions.
531
532 **Histology.** Whole lungs were harvested from groups of mice at 18 hours and at 48 hours
533 post co-infection and fixed in 10% neutral buffered formalin for 2 days. The tissues were
534 then embedded in paraffin, sectioned at 5 μm and stained with Hematoxylin and Eosin at
535 the Animal Histology Core at Tufts University. Sections of lung from three mice per group
536 were imaged using a Nikon Eclipse E400 microscope. Photomicrographs were captured
537 using a SPOT Idea 5.0-megapixel color digital camera and SPOT software.
538 Histopathologic scoring was performed by a board-certified anatomic pathologist
539 experienced in murine pathology, from 0 (no damage) to 4+ (maximal damage) for alveolar
540 congestion, hemorrhage, alveolar thickness, neutrophils, and lymphocytic infiltration (84).
541
542 **Cytokine Analysis.** Cytokines in the lungs and serum samples were measured using
543 Mouse Cytokine 8-Plex Array (Quanterix, Billerica, MA) following the manufacturer's
544 instructions. Frozen lung homogenates and serum samples were thawed on ice and mixed
545 by gentle vortexing. Levels in lung supernatants and serum samples were measured using
546 the Cirascan at the Imager at Tufts University Genomic Core (Boston, MA) and analyzed
547 by the Cirascan/Cirasoft program. Qlucore Omic Explorer (version 3.5) was used for the
548 generation of lung cytokine box plots. Concentrations of cytokines (IL-10, IL-2, IL-1β,
549 TNFα, IL-6, IFNγ, IL-17 and IL-12p70) were log-transformed, and displayed as Log_2 pg/ml.
550

551 **Statistical Analysis.** Statistical analysis was performed using Graph Pad Prism7. CFU
552 data were log-transformed to normalize distribution. Data are presented as mean values
553 +/- SEM. Significant differences ($p < 0.05$) were determined by Student's t-test. Differences
554 in fractions of mice that got sick were measured using Fisher's exact test. Survival analysis
555 was performed using the log rank (Mantel-Cox) test. Asterisks indicate significant
556 differences and *p* values are noted in the figures.
557

558 **ACKNOWLEDGEMENTS**

559 We would like to acknowledge James Nicholas Lee, Summer Schmaling, and Ognjen
560 Sekulovic for technical assistance with clinical score, virus preparation and nasal lavage
561 respectively. We would also like to thank Andrew Camilli for bacterial strains and Marta
562 Gaglia for protocols. They, along with Tim van Opijnen, Bharathi Sundaresh and Marcia
563 Osburne provided important feedback on the manuscript.
564

565 **FUNDING**

566 Research reported in this publication was supported by the National Institute On Aging of
567 the National Institutes of Health under Award Number R21 AG064215 to E.B.G. and F31
568 AI122615-01A1 to S.R.; King Abdullah Scholarship Program (KASP) implemented by the
569 Ministry of Higher Education (MOHE) under Award Number 7896504 to B.H.J.

570 **REFERENCES**

571 1. Kadioglu A, Weiser JN, Paton JC, Andrew PW. 2008. The role of Streptococcus
572 pneumoniae virulence factors in host respiratory colonization and disease. Nat Rev
573 Microbiol 6:288-301.
574 2. Chao Y, Marks LR, Pettigrew MM, Hakansson AP. 2014. Streptococcus
575 pneumoniae biofilm formation and dispersion during colonization and disease. Front
576 Cell Infect Microbiol 4:194.
577 3. Marks LR, Parameswaran GI, Hakansson AP. 2012. Pneumococcal interactions
578 with epithelial cells are crucial for optimal biofilm formation and colonization in vitro
579 and in vivo. Infect Immun 80:2744-60.
580 4. Marks LR, Davidson BA, Knight PR, Hakansson AP. 2013. Interkingdom signaling
581 induces Streptococcus pneumoniae biofilm dispersion and transition from
582 asymptomatic colonization to disease. MBio 4.
583 5. Blanchette-Cain K, Hinojosa CA, Akula Suresh Babu R, Lizcano A, Gonzalez-
584 Juarbe N, Munoz-Almagro C, Sanchez CJ, Bergman MA, Orihuela CJ. 2013.
585 Streptococcus pneumoniae biofilm formation is strain dependent, multifactorial, and
586 associated with reduced invasiveness and immunoreactivity during colonization.
587 MBio 4:e00745-13.
588 6. Boe DM, Boule LA, Kovacs EJ. 2017. Innate immune responses in the ageing lung.
589 Clin Exp Immunol 187:16-25.
590 7. Chong CP, Street PR. 2008. Pneumonia in the elderly: a review of the
591 epidemiology, pathogenesis, microbiology, and clinical features. South Med J
592 101:1141-5; quiz 1132, 1179.

593 8. Bogaert D, De Groot R, Hermans PW. 2004. Streptococcus pneumoniae
594 colonisation: the key to pneumococcal disease. Lancet Infect Dis 4:144-54.
595 9. Simell B, Auranen K, Kayhty H, Goldblatt D, Dagan R, O'Brien KL, Pneumococcal
596 Carriage G. 2012. The fundamental link between pneumococcal carriage and
597 disease. Expert Rev Vaccines 11:841-55.
598 10. Orsi A, Ansaldi F, Trucchi C, Rosselli R, Icardi G. 2016. Pneumococcus and the
599 Elderly in Italy: A Summary of Available Evidence Regarding Carriage, Clinical
600 Burden of Lower Respiratory Tract Infections and On-Field Effectiveness of PCV13
601 Vaccination. Int J Mol Sci 17.
602 11. Smith EL, Wheeler I, Adler H, Ferreira DM, Sa-Leao R, Abdullahi O, Adetifa I,
603 Becker-Dreps S, Esposito S, Farida H, Kandasamy R, Mackenzie GA, Nuorti JP,
604 Nzenze S, Madhi SA, Ortega O, Roca A, Safari D, Schaumburg F, Usuf E, Sanders
605 EAM, Grant LR, Hammitt LL, O'Brien KL, Gounder P, Bruden DJT, Stanton MC,
606 Rylance J. 2020. Upper airways colonisation of Streptococcus pneumoniae in adults
607 aged 60 years and older: A systematic review of prevalence and individual
608 participant data meta-analysis of risk factors. J Infect doi:10.1016/j.jinf.2020.06.028.
609 12. Regev-Yochay G, Raz M, Dagan R, Porat N, Shainberg B, Pinco E, Keller N,
610 Rubinstein E. 2004. Nasopharyngeal carriage of Streptococcus pneumoniae by
611 adults and children in community and family settings. Clin Infect Dis 38:632-9.
612 13. Flamaing J, Peetermans WE, Vandeven J, Verhaegen J. 2010. Pneumococcal
613 colonization in older persons in a nonoutbreak setting. J Am Geriatr Soc 58:396-8.
614 14. Palmu AA, Kaijalainen T, Saukkoriipi A, Leinonen M, Kilpi TM. 2012.
615 Nasopharyngeal carriage of Streptococcus pneumoniae and pneumococcal urine
616 antigen test in healthy elderly subjects. Scand J Infect Dis 44:433-8.

617 15. van Deursen AMM, van Houten MA, Webber C, Patton M, Scott D, Patterson S,
618 Jiang Q, Gruber WC, Schmoele-Thoma B, Grobbee DE, Bonten MJM, Sanders
619 EAM. 2018. The Impact of the 13-Valent Pneumococcal Conjugate Vaccine on
620 Pneumococcal Carriage in the Community Acquired Pneumonia Immunization Trial
621 in Adults (CAPiTA) Study. Clin Infect Dis 67:42-49.
622 16. Esposito S, Mari D, Bergamaschini L, Orenti A, Terranova L, Ruggiero L, Ierardi V,
623 Gambino M, Croce FD, Principi N. 2016. Pneumococcal colonization in older adults.
624 Immun Ageing 13:2.
625 17. van Deursen AM, van den Bergh MR, Sanders EA, Carriage Pilot Study G. 2016.
626 Carriage of Streptococcus pneumoniae in asymptomatic, community-dwelling
627 elderly in the Netherlands. Vaccine 34:4-6.
628 18. Krone CL, van de Groep K, Trzcinski K, Sanders EA, Bogaert D. 2014.
629 Immunosenescence and pneumococcal disease: an imbalance in host-pathogen
630 interactions. Lancet Respir Med 2:141-53.
631 19. Bou Ghanem EN, Clark S, Du X, Wu D, Camilli A, Leong JM, Meydani SN. 2015.
632 The alpha-tocopherol form of vitamin E reverses age-associated susceptibility to
633 streptococcus pneumoniae lung infection by modulating pulmonary neutrophil
634 recruitment. J Immunol 194:1090-9.
635 20. Bou Ghanem EN, Clark S, Roggensack SE, McIver SR, Alcaide P, Haydon PG,
636 Leong JM. 2015. Extracellular Adenosine Protects against Streptococcus
637 pneumoniae Lung Infection by Regulating Pulmonary Neutrophil Recruitment. PLoS
638 Pathog 11:e1005126.
639 21. Garvy BA, Harmsen AG. 1996. The importance of neutrophils in resistance to
640 pneumococcal pneumonia in adult and neonatal mice. Inflammation 20:499-512.

641 22. Hahn I, Klaus A, Janze AK, Steinwede K, Ding N, Bohling J, Brumshagen C,
642 Serrano H, Gauthier F, Paton JC, Welte T, Maus UA. 2011. Cathepsin G and
643 neutrophil elastase play critical and nonredundant roles in lung-protective immunity
644 against Streptococcus pneumoniae in mice. Infect Immun 79:4893-901.
645 23. Simell B, Vuorela A, Ekstrom N, Palmu A, Reunanen A, Meri S, Kayhty H,
646 Vakevainen M. 2011. Aging reduces the functionality of anti-pneumococcal
647 antibodies and the killing of Streptococcus pneumoniae by neutrophil phagocytosis.
648 Vaccine 29:1929-34.
649 24. Bhalla M SS, Abamonte A, Herring SE, Roggensack SE, Bou Ghanem EN. 2020.
650 Extracellular adenosine signaling reverses the age-driven decline in the ability of
651 neutrophils to kill S. pneumoniae. doi:https://doi.org/10.1101/2020.04.14.041418.
652 25. Pignatti P, Ragnoli B, Radaeli A, Moscato G, Malerba M. 2011. Age-related
653 increase of airway neutrophils in older healthy nonsmoking subjects. Rejuvenation
654 Res 14:365-70.
655 26. Menter T, Giefing-Kroell C, Grubeck-Loebenstein B, Tzankov A. 2014.
656 Characterization of the inflammatory infiltrate in Streptococcus pneumoniae
657 pneumonia in young and elderly patients. Pathobiology 81:160-7.
658 27. Bhowmick R, Tin Maung NH, Hurley BP, Ghanem EB, Gronert K, McCormick BA,
659 Leong JM. 2013. Systemic disease during Streptococcus pneumoniae acute lung
660 infection requires 12-lipoxygenase-dependent inflammation. J Immunol 191:5115-
661 23.
662 28. Rudra Bhowmick NM, Bryan Hurley, Karsten Gronert, Beth McCormick and John
663 Leong. 2012. Systemic disease during Streprococcus pneumoniae lung infection is
664 facilitated by hepoxilin A3 mediated nutophil recruitment, Submitted, In revision.

665 29. Bakaletz LO. 2017. Viral-bacterial co-infections in the respiratory tract. Curr Opin
666 Microbiol 35:30-35.
667 30. McCullers JA. 2006. Insights into the interaction between influenza virus and
668 pneumococcus. Clin Microbiol Rev 19:571-82.
669 31. Chertow DS, Memoli MJ. 2013. Bacterial coinfection in influenza: a grand rounds
670 review. JAMA 309:275-82.
671 32. Centers for Disease C, Prevention. 2010. Estimates of deaths associated with
672 seasonal influenza --- United States, 1976-2007. MMWR Morb Mortal Wkly Rep
673 59:1057-62.
674 33. Shrestha S, Foxman B, Weinberger DM, Steiner C, Viboud C, Rohani P. 2013.
675 Identifying the interaction between influenza and pneumococcal pneumonia using
676 incidence data. Sci Transl Med 5:191ra84.
677 34. McCullers JA. 2014. The co-pathogenesis of influenza viruses with bacteria in the
678 lung. Nat Rev Microbiol 12:252-62.
679 35. Palacios G, Hornig M, Cisterna D, Savji N, Bussetti AV, Kapoor V, Hui J, Tokarz R,
680 Briese T, Baumeister E, Lipkin WI. 2009. Streptococcus pneumoniae coinfection is
681 correlated with the severity of H1N1 pandemic influenza. PLoS One 4:e8540.
682 36. Dhanoa A, Fang NC, Hassan SS, Kaniappan P, Rajasekaram G. 2011.
683 Epidemiology and clinical characteristics of hospitalized patients with pandemic
684 influenza A (H1N1) 2009 infections: the effects of bacterial coinfection. Virol J
685 8:501.
686 37. Siegel SJ, Roche AM, Weiser JN. 2014. Influenza promotes pneumococcal growth
687 during coinfection by providing host sialylated substrates as a nutrient source. Cell
688 Host Microbe 16:55-67.

689 38. Rowe HM, Meliopoulos VA, Iverson A, Bomme P, Schultz-Cherry S, Rosch JW.
690 2019. Direct interactions with influenza promote bacterial adherence during
691 respiratory infections. Nat Microbiol 4:1328-1336.
692 39. Diavatopoulos DA, Short KR, Price JT, Wilksch JJ, Brown LE, Briles DE, Strugnell
693 RA, Wijburg OL. 2010. Influenza A virus facilitates Streptococcus pneumoniae
694 transmission and disease. FASEB J 24:1789-98.
695 40. Reddinger RM, Luke-Marshall NR, Sauberan SL, Hakansson AP, Campagnari AA.
696 2018. Streptococcus pneumoniae Modulates Staphylococcus aureus Biofilm
697 Dispersion and the Transition from Colonization to Invasive Disease. MBio 9.
698 41. McCullers JA, Rehg JE. 2002. Lethal synergism between influenza virus and
699 Streptococcus pneumoniae: characterization of a mouse model and the role of
700 platelet-activating factor receptor. J Infect Dis 186:341-50.
701 42. Levandowski RA, Gerrity TR, Garrard CS. 1985. Modifications of lung clearance
702 mechanisms by acute influenza A infection. J Lab Clin Med 106:428-32.
703 43. Pittet LA, Hall-Stoodley L, Rutkowski MR, Harmsen AG. 2010. Influenza virus
704 infection decreases tracheal mucociliary velocity and clearance of Streptococcus
705 pneumoniae. Am J Respir Cell Mol Biol 42:450-60.
706 44. McCullers JA, Bartmess KC. 2003. Role of neuraminidase in lethal synergism
707 between influenza virus and Streptococcus pneumoniae. J Infect Dis 187:1000-9.
708 45. Smith AM, McCullers JA. 2014. Secondary bacterial infections in influenza virus
709 infection pathogenesis. Curr Top Microbiol Immunol 385:327-56.
710 46. Cundell DR, Gerard NP, Gerard C, Idanpaan-Heikkila I, Tuomanen EI. 1995.
711 Streptococcus pneumoniae anchor to activated human cells by the receptor for
712 platelet-activating factor. Nature 377:435-8.

713 47. Ballinger MN, Standiford TJ. 2010. Postinfluenza bacterial pneumonia: host
714 defenses gone awry. J Interferon Cytokine Res 30:643-52.
715 48. Metzger DW, Sun K. 2013. Immune dysfunction and bacterial coinfections following
716 influenza. J Immunol 191:2047-52.
717 49. Sun K, Metzger DW. 2008. Inhibition of pulmonary antibacterial defense by
718 interferon-gamma during recovery from influenza infection. Nat Med 14:558-64.
719 50. Nakamura S, Davis KM, Weiser JN. 2011. Synergistic stimulation of type I
720 interferons during influenza virus coinfection promotes Streptococcus pneumoniae
721 colonization in mice. J Clin Invest 121:3657-65.
722 51. Cho SJ, Plataki M, Mitzel D, Lowry G, Rooney K, Stout-Delgado H. 2018.
723 Decreased NLRP3 inflammasome expression in aged lung may contribute to
724 increased susceptibility to secondary Streptococcus pneumoniae infection. Exp
725 Gerontol 105:40-46.
726 52. https://www.cdc.gov/flu/about/burden/index.html 2018. Disease Burden of
727 Influenza. CENTERS FOR DISEASE CONTROL AND PREVENTION.
728 53. Krone CL, Wyllie AL, van Beek J, Rots NY, Oja AE, Chu ML, Bruin JP, Bogaert D,
729 Sanders EA, Trzcinski K. 2015. Carriage of Streptococcus pneumoniae in aged
730 adults with influenza-like-illness. PLoS One 10:e0119875.
731 54. Aaberge IS, Eng J, Lermark G, Lovik M. 1995. Virulence of Streptococcus
732 pneumoniae in mice: a standardized method for preparation and frozen storage of
733 the experimental bacterial inoculum. Microb Pathog 18:141-52.
734 55. Tettelin H, Nelson KE, Paulsen IT, Eisen JA, Read TD, Peterson S, Heidelberg J,
735 DeBoy RT, Haft DH, Dodson RJ, Durkin AS, Gwinn M, Kolonay JF, Nelson WC,
736 Peterson JD, Umayam LA, White O, Salzberg SL, Lewis MR, Radune D, Holtzapple

737 E, Khouri H, Wolf AM, Utterback TR, Hansen CL, McDonald LA, Feldblyum TV,
738 Angiuoli S, Dickinson T, Hickey EK, Holt IE, Loftus BJ, Yang F, Smith HO, Venter
739 JC, Dougherty BA, Morrison DA, Hollingshead SK, Fraser CM. 2001. Complete
740 genome sequence of a virulent isolate of Streptococcus pneumoniae. Science
741 293:498-506.
742 56. Bou Ghanem EN, Maung NHT, Siwapornchai N, Goodwin AE, Clark S, Munoz-Elias
743 EJ, Camilli A, Gerstein RM, Leong JM. 2018. Nasopharyngeal Exposure to
744 Streptococcus pneumoniae Induces Extended Age-Dependent Protection against
745 Pulmonary Infection Mediated by Antibodies and CD138(+) Cells. J Immunol
746 200:3739-3751.
747 57. Bhalla M, Hui Yeoh J, Lamneck C, Herring SE, Tchalla EYI, Heinzinger LR, Leong
748 JM, Bou Ghanem EN. 2020. A1 adenosine receptor signaling reduces
749 Streptococcus pneumoniae adherence to pulmonary epithelial cells by targeting
750 expression of platelet-activating factor receptor. Cell Microbiol 22:e13141.
751 58. Rello J, Pop-Vicas A. 2009. Clinical review: primary influenza viral pneumonia. Crit
752 Care 13:235.
753 59. Torres A, Loeches IM, Sligl W, Lee N. 2020. Severe flu management: a point of
754 view. Intensive Care Med 46:153-162.
755 60. Boyd AR, Shivshankar P, Jiang S, Berton MT, Orihuela CJ. 2012. Age-related
756 defects in TLR2 signaling diminish the cytokine response by alveolar macrophages
757 during murine pneumococcal pneumonia. Exp Gerontol 47:507-18.
758 61. Thevaranjan N, Puchta A, Schulz C, Naidoo A, Szamosi JC, Verschoor CP, Loukov
759 D, Schenck LP, Jury J, Foley KP, Schertzer JD, Larche MJ, Davidson DJ, Verdu
760 EF, Surette MG, Bowdish DME. 2018. Age-Associated Microbial Dysbiosis

761 Promotes Intestinal Permeability, Systemic Inflammation, and Macrophage
762 Dysfunction. Cell Host Microbe 23:570.
763 62. McNamee LA, Harmsen AG. 2006. Both influenza-induced neutrophil dysfunction
764 and neutrophil-independent mechanisms contribute to increased susceptibility to a
765 secondary Streptococcus pneumoniae infection. Infect Immun 74:6707-21.
766 63. Bou Ghanem EN, Lee JN, Joma BH, Meydani SN, Leong JM, Panda A. 2017. The
767 Alpha-Tocopherol Form of Vitamin E Boosts Elastase Activity of Human PMNs and
768 Their Ability to Kill Streptococcus pneumoniae. Front Cell Infect Microbiol 7:161.
769 64. Gingles NA, Alexander JE, Kadioglu A, Andrew PW, Kerr A, Mitchell TJ, Hopes E,
770 Denny P, Brown S, Jones HB, Little S, Booth GC, McPheat WL. 2001. Role of
771 genetic resistance in invasive pneumococcal infection: identification and study of
772 susceptibility and resistance in inbred mouse strains. Infect Immun 69:426-34.
773 65. Kadioglu A, Andrew PW. 2005. Susceptibility and resistance to pneumococcal
774 disease in mice. Brief Funct Genomic Proteomic 4:241-7.
775 66. Bou Ghanem EN, Jones GS, Myers-Morales T, Patil PD, Hidayatullah AN, D'Orazio
776 SE. 2012. InlA promotes dissemination of Listeria monocytogenes to the mesenteric
777 lymph nodes during food borne infection of mice. PLoS Pathog 8:e1003015.
778 67. Kadioglu A, Cuppone AM, Trappetti C, List T, Spreafico A, Pozzi G, Andrew PW,
779 Oggioni MR. 2011. Sex-based differences in susceptibility to respiratory and
780 systemic pneumococcal disease in mice. J Infect Dis 204:1971-9.
781 68. Wagenvoort GH, Sanders EA, Vlaminckx BJ, de Melker HE, van der Ende A, Knol
782 MJ. 2017. Sex differences in invasive pneumococcal disease and the impact of
783 pneumococcal conjugate vaccination in the Netherlands, 2004 to 2015. Euro
784 Surveill 22.

785 69. Gutierrez F, Masia M, Mirete C, Soldan B, Rodriguez JC, Padilla S, Hernandez I,
786 Royo G, Martin-Hidalgo A. 2006. The influence of age and gender on the
787 population-based incidence of community-acquired pneumonia caused by different
788 microbial pathogens. J Infect 53:166-74.
789 70. Greene CJ, Marks LR, Hu JC, Reddinger R, Mandell L, Roche-Hakansson H, King-
790 Lyons ND, Connell TD, Hakansson AP. 2016. Novel Strategy To Protect against
791 Influenza Virus-Induced Pneumococcal Disease without Interfering with Commensal
792 Colonization. Infect Immun 84:1693-1703.
793 71. Mina MJ, Klugman KP, McCullers JA. 2013. Live attenuated influenza vaccine, but
794 not pneumococcal conjugate vaccine, protects against increased density and
795 duration of pneumococcal carriage after influenza infection in pneumococcal
796 colonized mice. J Infect Dis 208:1281-5.
797 72. Wadowsky RM, Mietzner SM, Skoner DP, Doyle WJ, Fireman P. 1995. Effect of
798 experimental influenza A virus infection on isolation of Streptococcus pneumoniae
799 and other aerobic bacteria from the oropharynges of allergic and nonallergic adult
800 subjects. Infect Immun 63:1153-7.
801 73. Jochems SP, Marcon F, Carniel BF, Holloway M, Mitsi E, Smith E, Gritzfeld JF,
802 Solorzano C, Reine J, Pojar S, Nikolaou E, German EL, Hyder-Wright A, Hill H,
803 Hales C, de Steenhuijsen Piters WAA, Bogaert D, Adler H, Zaidi S, Connor V,
804 Gordon SB, Rylance J, Nakaya HI, Ferreira DM. 2018. Inflammation induced by
805 influenza virus impairs human innate immune control of pneumococcus. Nat
806 Immunol 19:1299-1308.

807 74. Stout-Delgado HW, Vaughan SE, Shirali AC, Jaramillo RJ, Harrod KS. 2012.
808 Impaired NLRP3 inflammasome function in elderly mice during influenza infection is
809 rescued by treatment with nigericin. J Immunol 188:2815-24.
810 75. Gay R, Han SN, Marko M, Belisle S, Bronson R, Meydani SN. 2004. The effect of
811 vitamin E on secondary bacterial infection after influenza infection in young and old
812 mice. Ann N Y Acad Sci 1031:418-21.
813 76. Smith MW, Schmidt JE, Rehg JE, Orihuela CJ, McCullers JA. 2007. Induction of
814 pro- and anti-inflammatory molecules in a mouse model of pneumococcal
815 pneumonia after influenza. Comp Med 57:82-9.
816 77. McNeela EA, Burke A, Neill DR, Baxter C, Fernandes VE, Ferreira D, Smeaton S,
817 El-Rachkidy R, McLoughlin RM, Mori A, Moran B, Fitzgerald KA, Tschopp J, Petrilli
818 V, Andrew PW, Kadioglu A, Lavelle EC. 2010. Pneumolysin activates the NLRP3
819 inflammasome and promotes proinflammatory cytokines independently of TLR4.
820 PLoS Pathog 6:e1001191.
821 78. Pettigrew MM, Marks LR, Kong Y, Gent JF, Roche-Hakansson H, Hakansson AP.
822 2014. Dynamic changes in the Streptococcus pneumoniae transcriptome during
823 transition from biofilm formation to invasive disease upon influenza A virus infection.
824 Infect Immun 82:4607-19.
825 79. Siwapornchai N, Lee JN, Tchalla EYI, Bhalla M, Yeoh JH, Roggensack SE, Leong
826 JM, Bou Ghanem EN. 2020. Extracellular adenosine enhances the ability of PMNs
827 to kill Streptococcus pneumoniae by inhibiting IL-10 production. J Leukoc Biol
828 doi:10.1002/JLB.4MA0120-115RR.

829 80. Short KR, Reading PC, Wang N, Diavatopoulos DA, Wijburg OL. 2012. Increased
830 nasopharyngeal bacterial titers and local inflammation facilitate transmission of
831 Streptococcus pneumoniae. MBio 3.
832 81. Kulkarni U, Zemans RL, Smith CA, Wood SC, Deng JC, Goldstein DR. 2019.
833 Excessive neutrophil levels in the lung underlie the age-associated increase in
834 influenza mortality. Mucosal Immunol 12:545-554.
835 82. van der Sluijs KF, van Elden LJ, Nijhuis M, Schuurman R, Pater JM, Florquin S,
836 Goldman M, Jansen HM, Lutter R, van der Poll T. 2004. IL-10 is an important
837 mediator of the enhanced susceptibility to pneumococcal pneumonia after influenza
838 infection. J Immunol 172:7603-9.
839 83. Swamydas M, Lionakis MS. 2013. Isolation, purification and labeling of mouse bone
840 marrow neutrophils for functional studies and adoptive transfer experiments. J Vis
841 Exp doi:10.3791/50586:e50586.
842 84. Nishina K, Mikawa K, Takao Y, Shiga M, Maekawa N, Obara H. 1998. Intravenous
843 lidocaine attenuates acute lung injury induced by hydrochloric acid aspiration in
844 rabbits. Anesthesiology 88:1300-9.
845
846
847
848
849
850
851
852

853 **FIGURES & LEGENDS**

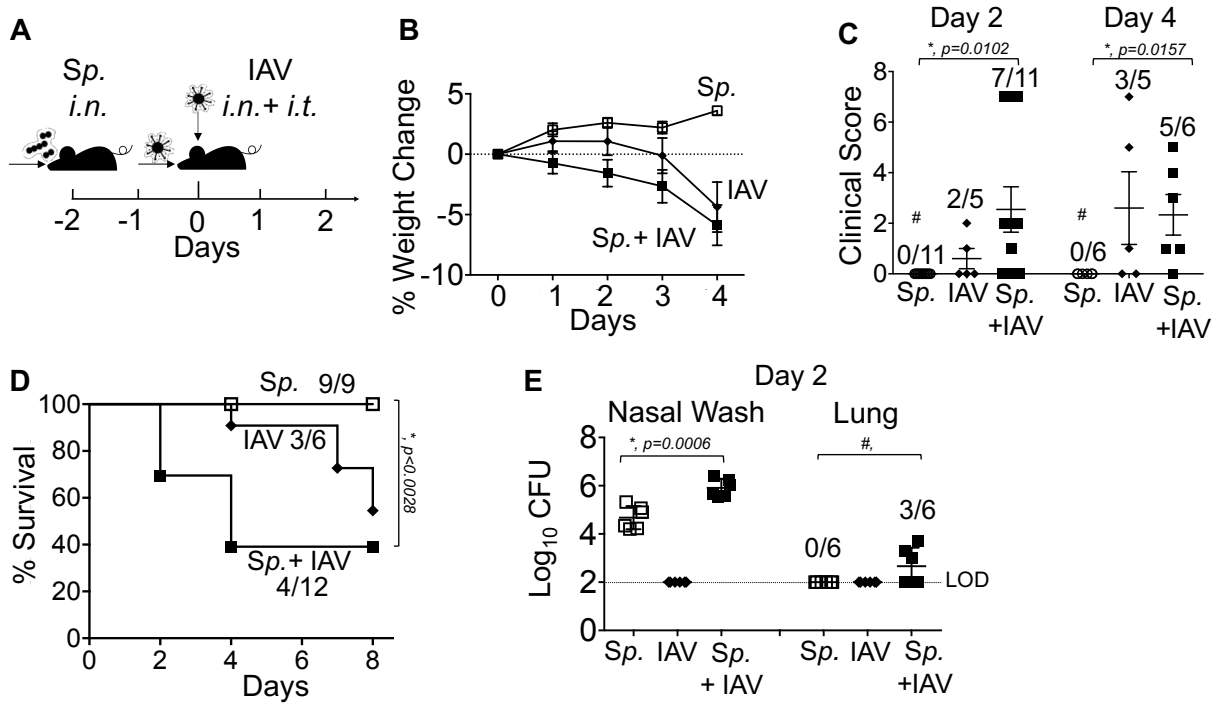

854

855 **Figure 1. Combined intranasal/intratracheal IAV inoculation of *S. pneumoniae*-**
856 **colonized mice results in bacterial dissemination and disease.** (A) Timeline of co-
857 infection; 8-10 weeks old male C57BL/6 (B6) mice were inoculated i.n. with $5x10^6$ CFU of
858 biofilm grown S. *pneumoniae* TIGR4 to establish colonization in the nasopharynx. 48 hours
859 later, the mice were either mock treated (*Sp*) or received 500 PFU of Influenza A virus PR8
860 (IAV) i.n. and 20 PFU i.t. (B) Percent weight loss was monitored daily. (C) Blinded clinical
861 scoring was performed on day 2 and day 4 post IAV infection. The fractions denote the
862 number of sick mice observed over total number of mice. A score of 0 means no sign of
863 sickness observed and a score above 1 indicates observable sickness. (D) Survival was
864 monitored for 8 days post IAV infection with fractions denoting survivors over total number
865 of mice. (E) The bacterial burden in the nasopharynx and lung were determined at day 2
866 post IAV infection. Pooled data from three separate experiments, n = 6-12 mice per group
867 are shown. Statistically significant differences determined by Student's t-test for bacterial

868 burden and clinical score and the log-rank (Mantel-Cox) test for survival are indicated by
869 asterisks. #, indicates statistical significance ($p < 0.05$) between *Sp* and *Sp*+IAV groups by
870 Fisher's exact test.
871
872
873
874
875
876
877
878
879
880
881
882

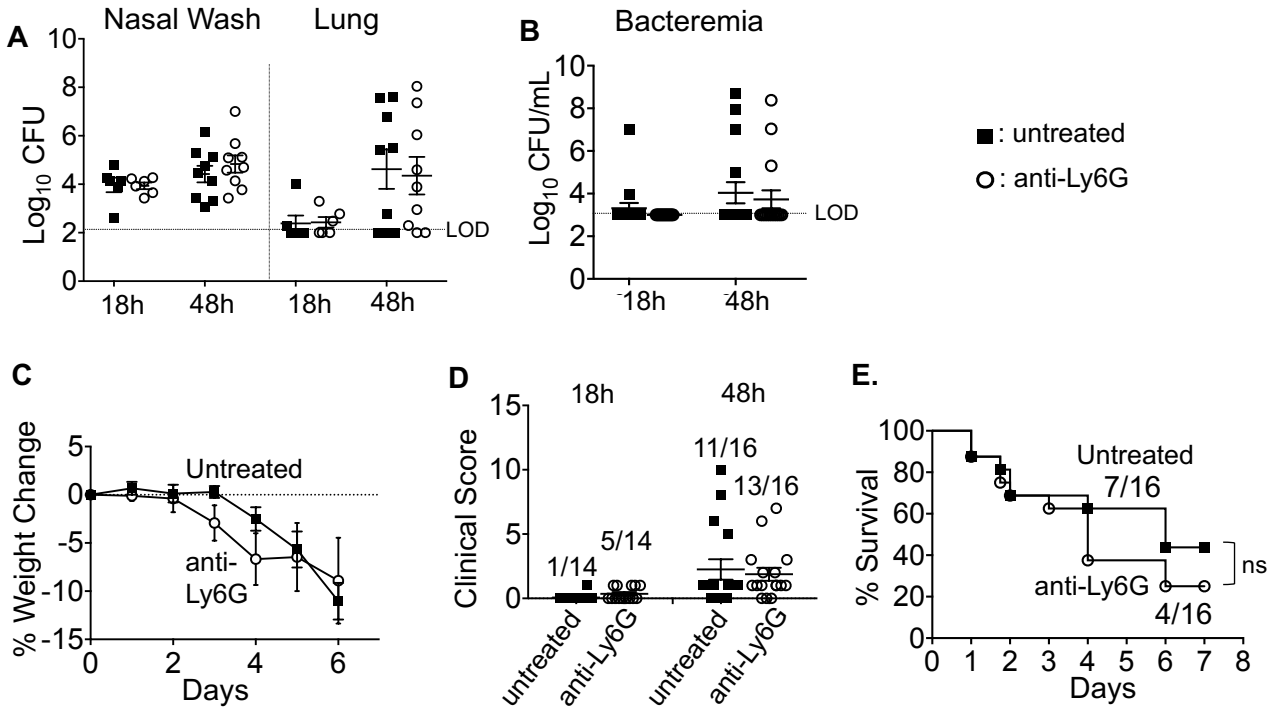

Figure 2. PMN depletion does not significantly affect the course of disease during IAV/*S. pneumoniae* co-infection. 8-10 weeks old C57BL/6 mice were intraperitoneally (i.p.) injected with anti-Ly6G (clone 1A8) antibodies to deplete neutrophils or mock treated. The antibodies were given daily from day -3 to day 1, and every other day from day 3 to the end of each experiment (with respect to IAV-infection). (A) At 18 and 48 hours post IAV infection, bacterial numbers in the nasal wash and lungs were determined. Bacteremia (B) and weight loss (C) was monitored over time. (D) Mice were blindly scored for symptoms of diseases at 18 and 48 hours post IAV-infection. The fractions indicate number of mice with clinical sickness (clinical score above 1) over total number of mice. (E) Survival was monitored over time where the fractions denote survivors over total number of mice at 8 days post IAV infection. Data shown represent the means +/- SEM and are pooled from three separate experiments with n=16 mice per group. Statistically significant differences were determined by Student's t-test for bacterial burden and clinical score and the log-rank (Mantel-Cox) and *ns* = not significant

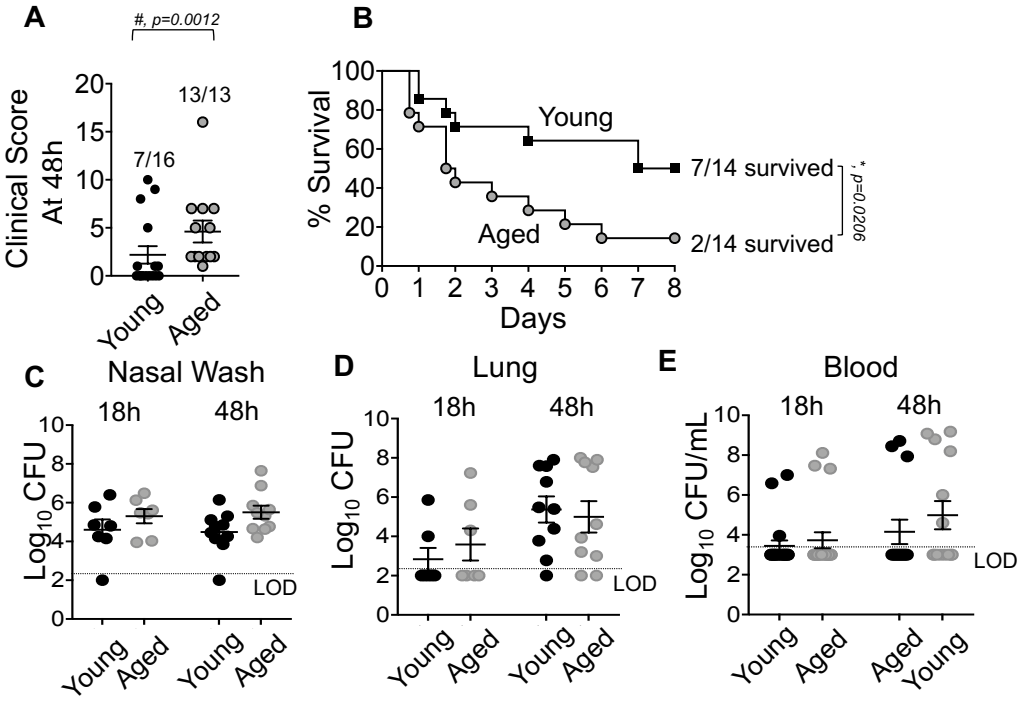

Figure 3. Aging increases susceptibility to IAV/*S. pneumoniae* co-infection. Young (8-10 weeks) and aged (18-24 months) C57BL/6 male mice were co-infected with *S. pneumoniae* TIGR4 i.n. and Influenza A virus PR8 i.n. and i.t. (as in Figure 1A). (A) Clinical score of co-infected young and aged mice at day 2 post IAV-infection is shown; the number of mice with demonstrable illness over total number of mice is indicated. Data shown are pooled from four experiments with n=13-16 mice per group. #, indicate statistical significance by Fisher's exact test. (B) Survival of co-infected young and aged mice were monitored over time with fractions denoting survivors over total of mice. Data are pooled from four experiments with n=14 mice per group. Asterisks indicate statistical significance by the log–rank (Mantel-Cox) test. (C-E) Bacterial burdens in the nasal wash, lungs, and blood were determined at 18 and 48 hours post IAV inoculation. The mean +/- SEM pooled from three separate experiments with n=7-10 mice per age group are shown. LOD denotes the limit of detection.

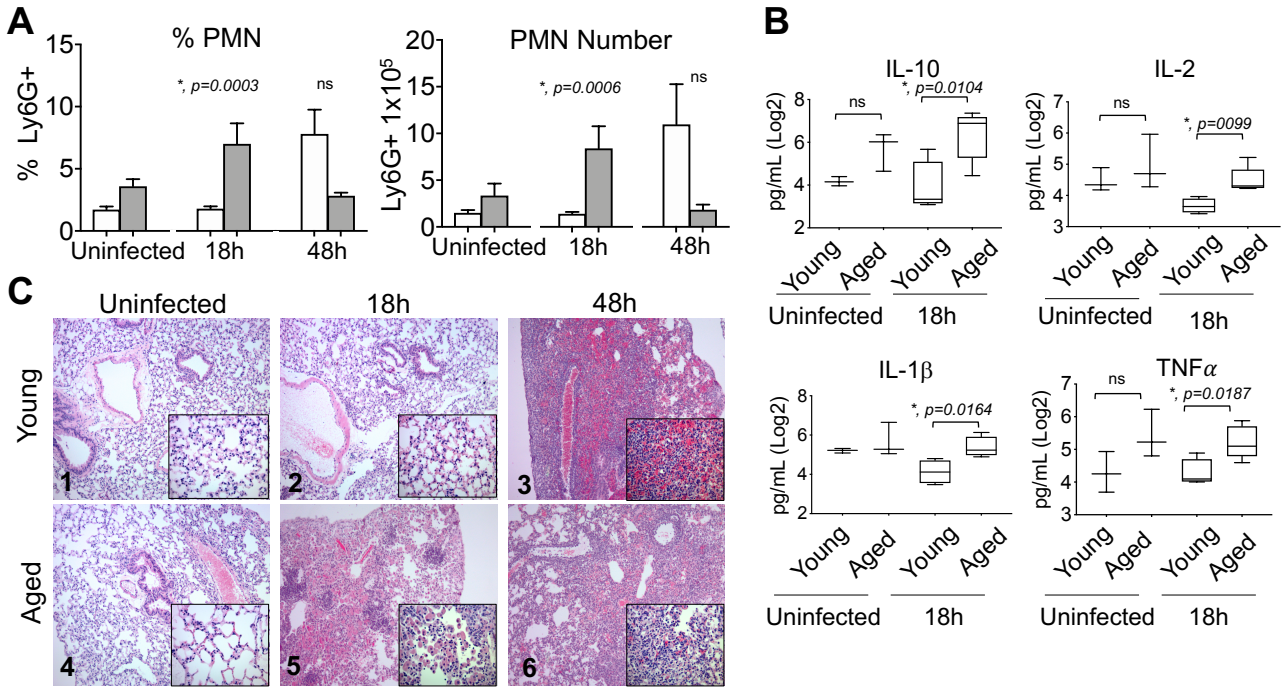

Figure 4. Aging is associated with more rapid lung inflammation. Young and aged C57BL/6 male mice were co-infected with S. *pneumoniae* and Influenza A virus PR8. 18 and 48 hours following IAV-infection (see experimental design in Fig. 1A), the lungs were harvested. (A) The percentages and total number of PMNs (Ly6G+) in the lungs was measured by flow cytometry. Young mice are represented by open bars and aged mice by shaded bars. The mean +/- SEM pooled from three separate experiments with n = 6 mice and n=12 mice per group at 18 and 48 hours respectively are shown. Statistically significant differences determined by Student's t-test are indicated by asterisks. (B) Cytokines in the supernatants of lung homogenates of young (n=4) or aged (n=5) mice at 18 hours post co-infection were measured by multiplex ELISA. Asterisks represent statistical significance by Student's t-test. (C) Lungs were stained with Hematoxylin and Eosin and shown are representative photographs at 100x and 400X are shown (inset)

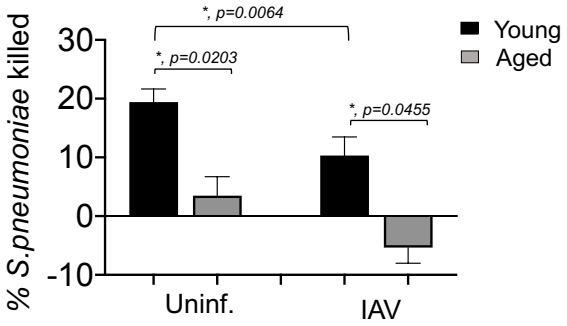

926

927 **Figure 5. Aging and IAV infection diminish the ability of PMNs to kill *S. pneumoniae***
928 ***ex vivo***. PMNs were isolated from bone marrow of young (8-10 weeks) and aged (18-24
929 months) C57BL/6 male mice that were mock-infected (uninf.) or singly infected with IAV
930 (i.n. + i.t.) for 2 days. PMNs were incubated with *S. pneumoniae* pre-opsonized with
931 homologous sera from the same mouse for 45 minutes at 37°C. The percentages of *S.*
932 *pneumoniae* killed upon incubation with PMNs were determined with respect to a no PMN
933 control. Data shown represent the means +/- SEM pooled from two experiments (n=3 mice
934 per group) where each condition was tested in quadruplicates per experiment. Asterisks
935 represent statistical significance as determined by Student's t-test.

936